Polymer 221 (2021) 123626

Contents lists available at ScienceDirect

Polymer

journal homepage: http://www.elsevier.com/locate/polymer

Utilization of ABS from plastic waste through single-step reactive extrusion of LDPE/ABS blends of improved properties

Dipti Saxena, Pralay Maiti *

School of Materials Science and Technology, Indian Institute of Technology (Banaras Hindu University), Varanasi 221005, India

ARTICLE INFO

Keywords:
Recycling
Microstructural analysis
Strength
Extrusion

ABSTRACT

Chemical mixture (C-M) of low density polyethylene (LDPE) and electronic waste made of acrylonitrile butadiene styrene (ABS) have been prepared via one step reactive extrusion. The morphology of prepared crosslinked blends has been investigated. Single phase morphology has been found in C-M as opposed to two phase morphology in physical blend. The extent of crosslinking has been observed by determining gel content through solvent extraction. The structural changes have been confirmed by FTIR and solid state ^{13}C NMR spectroscopy. The C-M have been tested using DSC and TGA and have found to be thermally stable. The chemical mixture has showed excellent mechanical properties like increment in Young's modulus, ultimate tensile strength. The flexural properties have also been investigated and C-M has found to have enhanced flexural modulus and flexural stress. For C-M to be used in practical heat exposure conditions heat distortion temperature tests have been performed and C-M has shown better properties than pure LDPE and physical blend.

1. Introduction

As polymers are an inherent part of our lives today, there is an urgent need to recycle and reuse them and obviously there is a prerequisite to enhance their properties for different applications. Continuous research is going on to produce high performance polymeric materials to incorporate wide array of properties. Plastic plays a crucial role in our day to day lives as we are highly dependent on different products made out of it. Massive production of plastics is underway to fulfil the demands of the society every year. The discarded plastic products after use, creates a humongous amount of plastic waste which is increasing day by day. The harmful chemicals present in the plastic waste can disrupt water, soil as well as widely diverse wildlife and create other environmental problems. So, there is a strong necessity to reuse and utilize them in an effective manner to curb the amount of discarded plastic waste. Using them as polymer blends and composites to enhance the properties of some of the existing polymers can prove to be a great way to regulate them again in practical lives.

The useful portion of discarded plastics can also be utilized to enhance the properties of some existing polymers. Poly (acrylonitrile-butadiene-styrene) (ABS) is largely present in the discarded electronic waste. ABS is a preferred polymer in applications in electronics as well as in automotive industry due to its excellent mechanical properties and good surface finish. The properties can be customized by varying its constituents. It provides desirable properties along with ease of processing at a low cost. Low density polyethylene (LDPE), on the other hand, is a widely used polymer in applications such as in packaging, textile, construction and various other household items [1]. Continuous investigation has been going on for the improvement of its properties [2–9].

To incorporate the desirable properties, there arises a need to improve the belongings for different specific applications. Making polymer composites by using different kinds of filler is a well-known method to improve various properties such as structural, thermal, mechanical, gas barrier as well as in the field of biomedical, fuel cell applications etc. [10–16]. Other popular technique is to combine different polymers for the required purpose and making polymer blends. The polymer blends have been a widely studied research area. Two or more polymers are combined to modulate and enhance different properties [17–24]. Polymers having different polarity, which are immiscible as well, needs an additional agent to improve their interfacial interactions [17,18]. Various kinds of compatibilizers such as LDPE-g-MAH [9], SEBS-g-MAH (styrene-ethylene-styrene copolymer-grafted-maleic anhydride) [18], PP-g-MAH (polypropylene-grafted-maleic anhydride) [21], SEBS [22], PP-g-styrene-*co*-acrylonitrile [23], have been used in the past to improve the morphological, mechanical and other properties

* Corresponding author.
E-mail address: pmaiti.mst@itbhu.ac.in (P. Maiti).

https://doi.org/10.1016/j.polymer.2021.123626
Received 19 December 2020; Received in revised form 10 February 2021; Accepted 7 March 2021
Available online 11 March 2021

of the blends. Use of compatibilizers improve the mechanical properties, reduce the dispersed phase size, improve the interfacial adhesion up to a considerable extent. But the compatibilizers are synthesized separately which makes the overall process more energy consuming which is commercially undesirable.

Reactive extrusion has been the other technique to prepare polymer blends. In this approach, two polymers and copolymers or functionalized polymers are fed into the extruder and the reaction takes place within the extruder itself [6,24–26]. There are two types of reactive extrusions reported; one where the size of dispersed phase is reduced and the reactive agent provides compatibilization and in some reports the reactive extrusion causes crosslinking reactions in the polymer blends which is confirmed by gel content or gel fraction. Vadori et al. studied the reactive extrusion of poly (lactic acid) and ABS blends by using two additives (acrylic copolymer and joncryl) [24]. The morphology of the polymer blend was not changed drastically but the size of the dispersed ABS was reduced and the two-phase morphology persisted. There was improvement in toughness but tensile properties were not improved. Wang et al. introduced a two-step crosslinking process for the blends of polystyrene and LDPE [6]. LDPE was partially crosslinked first by using dicumyl peroxide. Then the crosslinked LDPE was melt blended with polystyrene in second step. Styrene-butadiene-styrene was added later in the second step. Mechanical properties were improved due to crosslinking between the two phases. ABS has been used in many studies for making polymer blends for various purposes [3,17,18,24–27]. There have not been enough research articles on LDPE/ABS system except few [3,22,27] due to the fact that the two polymers are highly immiscible and there is a need to modify the blend system. In this study, a one-step reactive extrusion process has been explored to produce a single-phase crosslinked chemical mixture (C-M) of LDPE and ABS in the form of electronic waste. The C-M has been tested for morphological, mechanical, thermal and heat distortion properties for its applications of reusing plastic e-waste.

2. Experimental

Materials: The polyethylene used was commercial grade low-density polyethylene (LDPE) which was obtained from Reliance Industries Ltd., India. The poly (acrylonitrile-butadiene-styrene) (ABS)was obtained from the e-waste collected from local sources. Maleic anhydride (MA) was purchased from Sigma Aldrich Chemical Pvt. Limited, having density of 98.06 g/mol.

Preparation of materials: For obtaining the ABS, parts of e-waste (such as computer keyboards, mouse etc) were collected from different sources. These parts were then washed thoroughly to get rid of any dust particles. After drying them, they were dried in air for 24 h and then vacuum dried for another 24 h. The parts were then cut into small pieces and grinded in mechanical grinder for turning them into fine powder. This ABS powder was used for further processing. LDPE granules were also grinded in mechanical grinder for making its fine powder.

Sample preparation: The polymer blends were prepared by melt extrusion technique in twin-screw extruder (Hakke Mini Lab). Fine powder of LDPE and ABS were mixed with MA in different proportions. The optimum ratio of polymers and MA with most favourable temperature conditions were obtained after preparing and testing the blends with varying MA concentration (Supplementary Fig. S1), varying PE and ABS concentrations (Supplementary Fig. S2) and varying operating temperatures (Supplementary Fig. S3). Hence, the optimum ratio taken here is PE:ABS as 75:25, MA concentration as 5 wt% and operating temperature as 220 °C. All powders were vacuum dried for 24 h prior to mixing. The blends were processed at a temperature of 220 °C, 100 rpm and a duration of 10 min. Simple mixing of two polymers will be termed as physical mixture (P-M) and the blends containing 5% of MA will be termed as chemical mixture (C-M) where both blends have 75:25 ratio of PE and ABS. The extruded blends were then made into thin sheets (~20 μm) using compression molding machine (S. D. Scientific Ltd.). These sheets were used for solvent extraction and polarized optical microscopy experiments. The dog bone specimens were also prepared for the mechanical testing using injection molding machine (Haake microinjector). The polymer blends were heated at 230 °C in the heating barrel. The mold temperature was kept at 40 °C. The material was injected at a pressure of 110 bar. The dimension of hence prepared dog bone samples was: thickness 2.12 mm, gauge length 20 mm and width of 4 mm.

2.1. Characterization

Scanning electron microscopy (SEM): SEM (SUPRA 40, Zeiss) was used to further investigate the morphology of fractured surfaces of pure and melt blended samples. The surface to be examined was gold coated by a sputtering apparatus prior to the inspection in SEM.

Atomic force microscopy (AFM): To study the surface roughness, atomic force microscopy was performed. An NT-MDT multimode scanning probe microscope having model NTEGRA Prima was used in semi contact mode. The tip used was of silicon nitride mounted on a long cantilever having frequency of 240–250 kHz and the spring constant was 11.5 N/m.

Gel content by solvent extraction: To determine the gel content which is indicative of crosslink density of the polymer blends, solvent extraction experiments were performed. The samples were dipped in solvents of PE and ABS to determine the dissolved percentage of the polymer blends. The samples were cut in a dimension of 1.5 × 1.5 cm^2 having thickness of 20 μm. The samples were weighed before dipping into any solvent. The samples then dipped and stirred in chloroform (solvent of ABS) for 24 h. After 24 h, samples were removed from the solvent and dried in air for 12 h and in vacuum for another 12 h. After that the weight difference was measured. Again the sample was dipped and stirred in xylene (solvent of PE) and the same procedure was repeated. The weight difference was used to determine the crosslinking percentage of the polymer blend.

$$Gel\ content\ (\%) = \frac{W_f}{W_i} \times 100 = \ indicative\ crosslink\ density\ (CDi)$$

Where, W_f is the weight after solvent extraction and W_i is the initial weight.

Polarized optical microscopy (POM): To determine the morphology and phase investigations, the thin sheets of samples were investigated by polarized optical microscopy (Leitz Biomed). Thin sheets of pure polymer and blends were tested to identify the different phases, level of mixing etc.

Fourier transform infrared spectroscopy (FTIR): FTIR spectra were obtained by using an α Bruker Eco-ATR which was furnished with ZnSe ATR crystal. The spectra were recorded in a range of 600–4000 cm^{-1} where resolution was kept at 4 cm^{-1} and number of scans of 100. The measurements were taken at room temperature. The sample thickness was kept approximately 100 μm.

Nuclear magnetic resonance spectroscopy (NMR): The measurements of solid state ^{13}C NMR were performed at a resonance frequency of 100 MHz on JEOL 400 MHz. The spinning probe used was 4 mm cross-polarization double resonance magic angle probe. For the measurements, weight of 100–200 mg of each sample was taken and tightly packed into a cylindrical zirconium oxide rotor of 4 mm using a kel-F end-cap.

Differential scanning calorimetry (DSC): The melting behaviour of polymer blends was analysed by differential scanning calorimetric experiment using Mettler 832. The DSC instrument was calibrated with zinc (for high temperatures) and indium (for low temperatures) before starting the measurements. The samples were kept in a platinum crucible of 70 μl. The experiments were performed at a temperature range of 25–200 °C after quenching the samples. The heating rate was kept at 10°/min.

Thermogravimetric analysis (TGA): Thermogravimetric analysis was done to determine the thermal stability and degradation temperatures of polymer blends. TGA was done using a thermogravimetric analyser (Mettler-Toledo) fitted with differential thermal analyser. The samples were heated in an alumina crucible. The measurements were taken from room temperature to 600 °C. The heating rate was kept 20°/min. The experiments were performed in an inert atmosphere and controlled flow rate of nitrogen.

Mechanical properties: The mechanical properties were determined using a universal testing machine. The experiments were performed in tensile mode using Instron universal testing machine (model: Instron 3369; load cell capacity 50 kN). The measurements were conducted at room temperature. The dog bone samples prepared by injection molding were stretched till the fracture occurred. Chuck distance was taken ~34 mm. The dog bone sample had gauge length of 20 mm, width of 4 mm and thickness of 2.14 mm (Supplementary Fig. S4). The samples were stretched at a constant strain rate of 5 mm/min. For minimum error estimation, three samples were tested for each composition of polymer blend. 3-point bending tests were performed on the same machine with 3-point bending jaws setup. The span length was taken as 20 mm. The constant strain rate was taken as 3 mm/min. Flexural stress (σ_f), flexural strain (ε_f) and flexural modulus (E), were

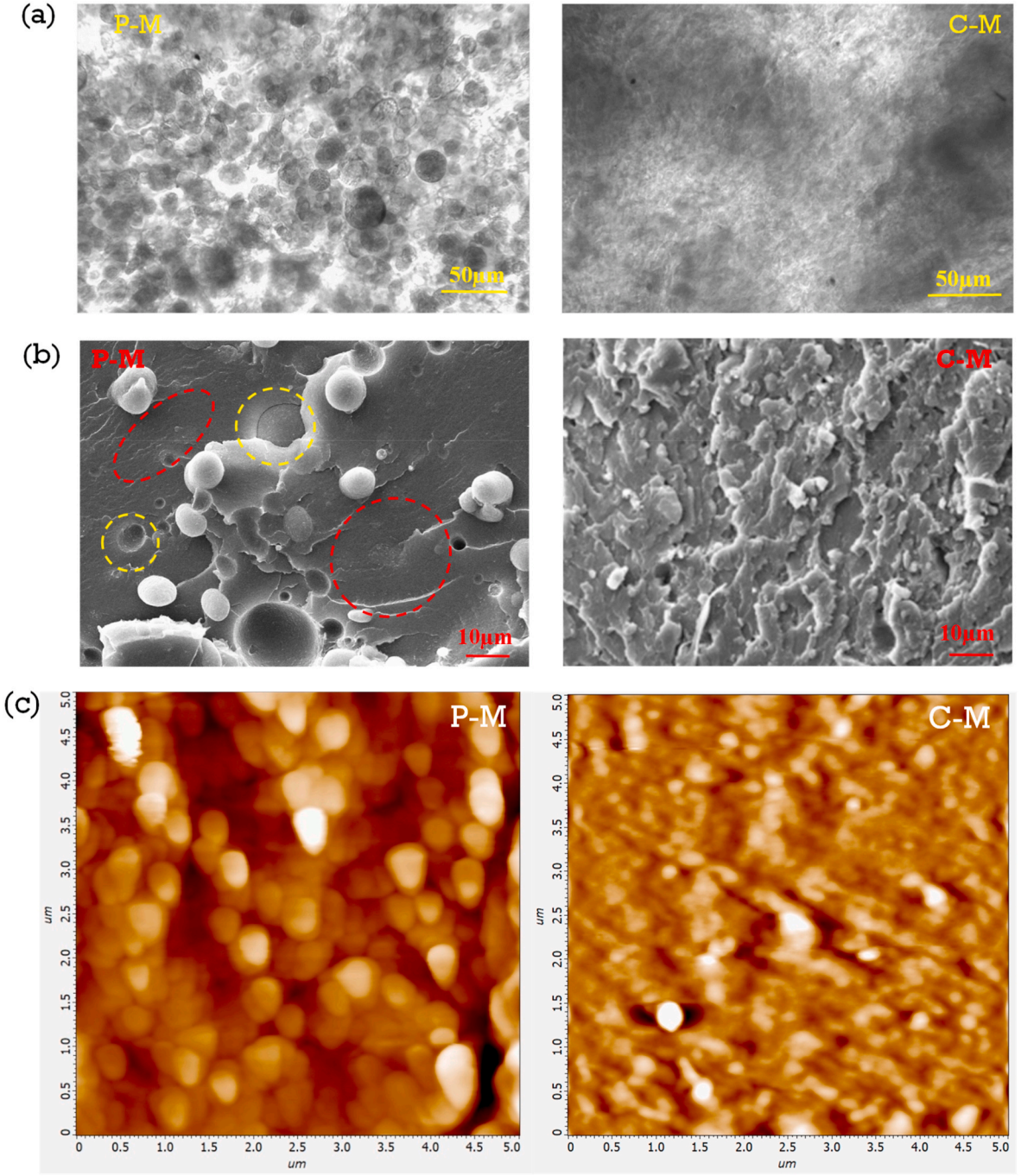

Fig. 1. (a) POM images of physical mixture (P–M) and chemical mixture (C–M) of ABS and PE; (b) SEM images of P-M and C-M, yellow dotted circles in the SEM image of P-M shows the embedded ABS particle in the PE matrix and the indentation left by ABS particle, red dotted circles represent the plain fractured surface of PE having no or fewer cracks present; and (c) AFM images of P-M and C-M showing relative roughness of surfaces of blends. (For interpretation of the references to colour in this figure legend, the reader is referred to the Web version of this article.)

calculated as:

$$\sigma_f = \frac{3FL}{2bd^2}$$

$$\varepsilon f = \frac{6\,Dd}{L^2}$$

$$E = \frac{L^3 m}{4bd^3}$$

where, F is load (N), L is support span length (mm), b and d are the width and thickness of the specimen (mm). D is the maximum deflection at the centre of the specimen (mm), m is the slope of the initial straight part of the flexural stress vs. flexural strain curve.

Dynamic Mechanical Analysis (DMA): Dynamic mechanical properties of the samples were performed on a dynamic mechanical analyser MCR 702 Multi Drive Anton Paar. The samples' dimensions were taken as $20 \times 5\ mm^2$ having a gauge length of 20 mm and thickness of 1 mm. The samples were tested in torsion mode at a frequency of 1 Hz, temperature range of −50° to 100 °C at a heating rate of 5°/min and strain of 0.05%.

Heat distortion temperature (HDT): Heat distortion temperature tests were conducted to ensure the applicability of the polymer blends to be able to work under different temperature range for specific weight loading condition. The HDT test was performed on a sample size of $20 \times 4 \times 2\ mm^3$ with span length of 20 mm. The 3-point bending arrangement was kept in a water bath. The load applied was 0.2 kgf. The temperature of water bath was increased gradually while applying the constant load till the sample deflects by a distance of 0.25 mm. The temperature of this deflection point was noted as heat distortion temperature (HDT).

3. Results and discussion

Phase morphology: Two immiscible polymers are phase segregated leading to two separate phases. As a result, there is insignificant property development out of mixing the two immiscible polymers. Fig. 1a shows the polarized optical micrographs of physical mixture (P-M) and chemical mixture (C-M). The POM images were taken in transmittance mode. The micrograph of P-M shows the two phase system where one phase of ABS is dispersed in the PE matrix. ABS polymer has somewhat spherical morphology which is heterogeneously distributed throughout the polymer blend. On the other hand, the micrograph of C-M exhibits a single-phase morphology which indicates better miscibility of the two polymers. The maleic anhydride (MA) acts as the bonding agent which chemically crosslink the polyethylene (PE) and ABS molecules which eventually convert it into single phase system. Further, the polar interactions between the two polymers enhance in presence of MA. Fig. 1b shows the SEM images of the fracture surfaces of physical (P-M) and chemical mixture (C-M). It is clearly seen from the SEM images that the P-M has a distinct two-phase morphology where the ABS particles are dispersed homogeneously in polyethylene matrix. The two phases are debonded, as shown in figure through circles. This debonding occurs due to low interfacial interaction between the two immiscible polymers. The poor miscibility arises due to different polarity of the two polymers. However, the two polymers are highly immiscible causing the separation of ABS particles in the form of spherical blobs in polyethylene matrix. On contrary, the chemical mixture (C-M) exhibits clear single-phase morphology. There is co-continuous type morphology present in C-M. The presence of MA creates crosslinking through reactive extrusion which convert it in a single-phase morphology. The smooth surface with fewer cracks represents the effortless debonding in the P-M while rough fracture surface in C-M indicates better adhesion between the two components. Therefore, the developed C-M system has better morphological properties as compared to physical mixture due to chemical crosslinking [4,6]. AFM is a tool to understand the roughness of the samples along with morphology. It is useful in determining the topographic or morphological changes as it can examine the morphology at very high spatial resolutions and area of micrometres to sub-nanometres can be scanned to examine the topography. The AFM images of $5 \times 5\ \mu m^2$ area of P-M and C-M have been shown in Fig. 1c. P-M shows globular morphology with the surface having distinct particle like impressions distributed all over the surface, further demonstrate the immiscible ABS particles in PE matrix in the blend. On the other hand, the chemical mixture shows the smoother surface comparatively. The morphology does not show the distinct particulate patterns in the C-M as evident from the surface roughness of 16.5 nm as opposed to overall surface roughness of 24.7 nm in P-M. The smoother surface results from the chemical bonding caused by the crosslinking between ABS and PE through reactive extrusion in presence of maleic anhydride. Hence, the crosslinking structure during reactive extrusion diminished the immiscibility or in other words enhanced the miscibility of two incompatible polymers like ABS and PE [5].

3.1. Gel content through solvent extraction (indicative crosslinking density, CD_i)

The solvent extraction has been performed to determine the gel content which gives the extent of crosslinking in the samples. Fig. 2a shows the photographic images of P-M and C-M specimens before and after the solvent extraction (in chloroform, solvent for ABS) and xylene (solvent for PE)) with remaining weight percentage after each step. The samples of physical mixture are put in chloroform for 24 h. After 24 h, the samples are taken out from the chloroform and dried thoroughly. The weight difference before and after dipping in chloroform results in 14% weight reduction. After drying, the samples are put in xylene at a temperature of 140 °C under stirring condition. All the samples get dissolved in the solvent within 5 min. This signifies that there is no crosslinking in the prepared physical mixture. The chloroform dipping results in only 14 wt% of the ABS removal from P-M present on the surface. Remaining ABS is surrounded mostly by PE which chloroform could not dissolve. When the samples are put in xylene, they get dissolved in xylene despite having the tiny ABS particle in it. On the other hand, the chemical mixture which contains 5 wt% MA are also put in the respective solvents of both the polymers for 24 h each. After chloroform dipping for 24 h, the weight difference is ~9%. After that the samples are dipped in xylene. The samples do not dissolve completely, rather 45% of the initial weight remains. This signifies that there is chemical bonding (crosslinking) between the two polymers due to which the resulting blend does not dissolve completely and the remaining undissolved 45% is considered as the extent of crosslinking in C-M blend. The images of samples before and after each solvent extraction have been shown in Fig. 2b and **c** through optical images and SEM, respectively. Polarized optical microscopic images have shown the visible pitting in P-M sample after solvent extraction using chloroform and the sample gets dissolved completely after putting in xylene. The C-M blend, however, shows less surface pitting as compared to P-M sample. The C-M specimen does not dissolve completely rather show considerable erosion of the surface due to solvent extraction using chloroform and xylene. SEM images in Fig. 2c also show the similar surface morphologies of samples of P-M and C-M before and after solvent extraction. The surface of samples before solvent dipping is quite uniform. After putting the P-M blend in chloroform, it shows rough and uneven surface because of the erosion of ABS from the surface while it gets dissolved completely in xylene. The sample of C-M also has an even surface before any solvent extraction while fewer pittings are observed after dipping in chloroform. It is clear that the surface erosion in C-M specimen is distinctly lesser than the P-M sample. The surface of C-M becomes more rough and uneven after dipping the sample in xylene because of 55% extraction of the polymers. However, solvent extraction studies confirm the crosslinking in C-M in presence of maleic anhydride as opposed to the complete dissolution of physical mixture.

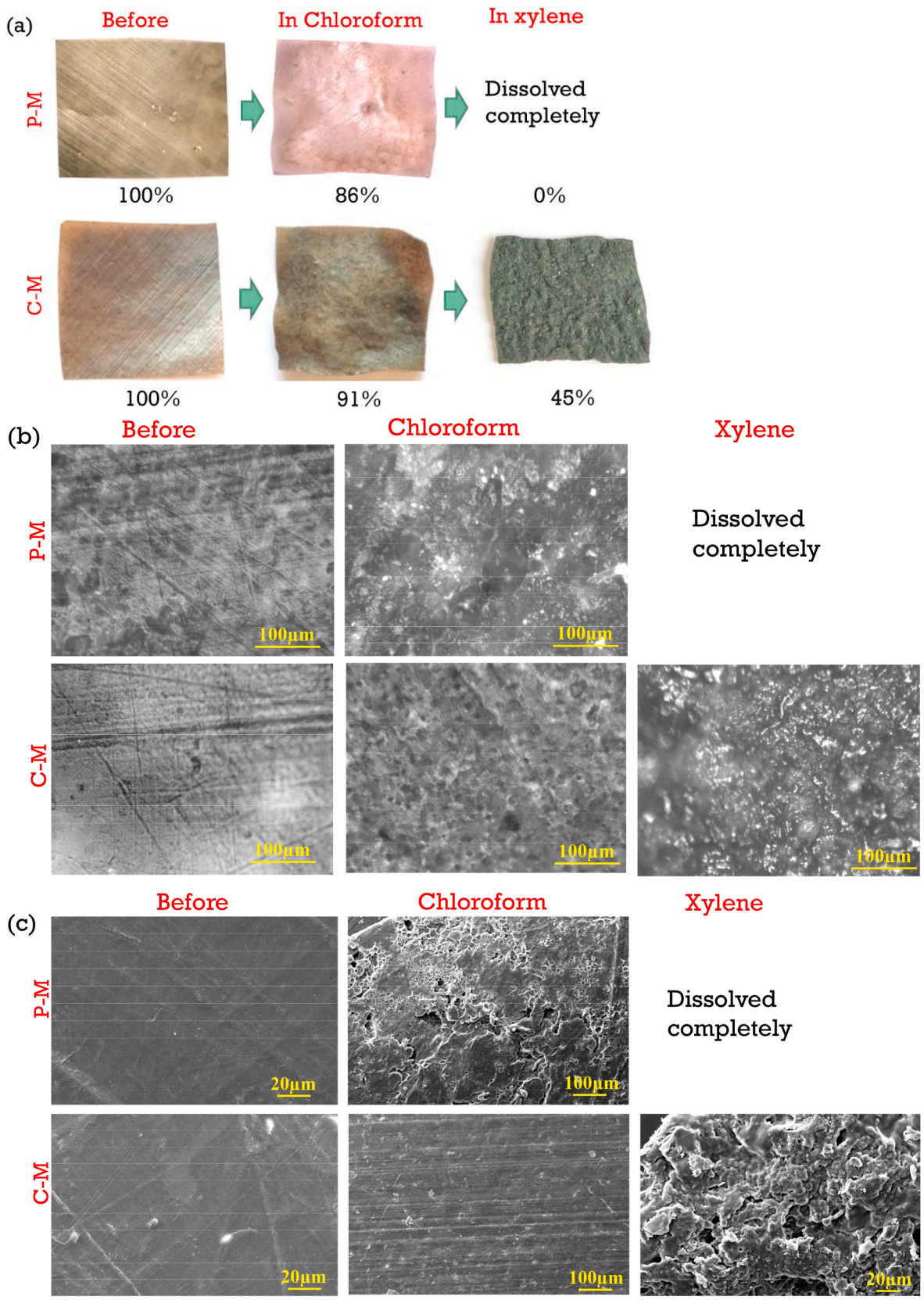

Fig. 2. (a) Photographic images of samples before and after the indicated solvent extraction, below each image, the percentage weight remained after each solvent extraction is mentioned; (b) Optical microscopic images in reflectance mode of the samples before and after solvent extraction; and (c) SEM images of samples before and after solvent extraction.

3.2. Proof of crosslinking and determination of its site

Morphology and solvent extraction studies indicate the possible crosslinking between the components (PE and ABS) and spectroscopic techniques are employed to visualise the chemical bonding. Fig. 3a shows the FTIR spectroscopic patterns of pure polymers and their physical and chemical blends. Polyethylene shows the characteristic peaks at 2914 and 1462 cm^{-1} corresponding to the C–H stretching and bending of normal alkene, respectively. The peak at 718 cm^{-1} signifies CH_2 rocking [5]. The FTIR spectra of ABS show a stretching band of C≡N group at 2236 cm^{-1}. The ring modes of styrene show peaks at 1600 $cm^{-1}$and 1492 cm^{-1}. The peak at 1451 cm^{-1} is due to the scissoring mode of CH_2 groups. Peaks at 965 $cm^{-1}$and 909 cm^{-1} arise due to the C–H deformation of the hydrogen attached with the alkene carbons. These distinct peaks are taken as the representatives of butadiene component. The peaks appear at 758 and 698 cm^{-1} signify the intense ring bending [28] and no change of peak positions is observed in physical mixture confirm insignificant interactions between the components, which led the system to immiscible one. On contrary, a new FTIR peak at 1768 cm^{-1}appears in chemical blend (C-M), corresponds to the carbonyl group due to the presence of maleic anhydride, indicating possible linking of PE and ABS through MA. There is another new peak in C-M at 1015 cm^{-1} which corresponds to the C–*O*–C linkage [29]. These two new peaks indicate that the maleic anhydride form the crosslinking with the base polymers. Further, there are considerable shift of peak positions in C-M as compared to their respective pure polymers and P-M such as the peaks at 965 cm^{-1} shifts to 967 cm^{-1}, the intense ring bending peaks at 758 and 697 cm^{-1} shift to 759 and 699 cm^{-1}. All these shifts signify the enhanced interactions between the two polymers in the chemical blend and turn into a single phase in maleic anhydride induced crosslinked blend.

Fig. 3b shows the solid state ^{13}C NMR spectra of physical and chemical mixture. A new signal at 47.04 ppm appears in C-M which is not present in physical mixture. This peak is deconvoluted to get the exact peak position as shown in the inset of Fig. 3b. This signal has emerged due to the attachment of MA with the main chains in the form of succinic anhydride as shown in inset of Fig. 3b (the carbon atom to which the peak at 47.04 is assigned has been marked by the dotted circle). However, the chemical crosslinking in presence of maleic anhydride is confirmed through spectroscopic techniques indicating the position of carbon site of crosslinking between PE and ABS through MA. The reaction mechanism of physical and chemical blends have been shown in Fig. 3c, where only physical intermixing of molecules occur in P-M while crosslinking between PE and ABS ensue through maleic anhydride in the phases and thereby enhance the interfacial interaction through reactive extrusion [30,31].

3.3. Thermal properties

To remove the thermal history, the samples are first heated from room temperature to 200 °C at a heating rate of 10°/min followed by quenching at a cooling rate of 40°/min. The second heating was then performed at a heating rate of 10°/min. Fig. 4a shows the DSC thermograms and the values obtained from DSC studies are presented in Table 1. PE sample shows a melting peak at 108.5 °C while the physical mixture indicates a melting point at 107 °C, and the decreases of melting temperature is due to dilution effect. The solvent extracted crosslinked portion was used for the DSC measurement of C-M. The melting of C-M occurs at 105.5 °C. E-waste ABS shows a glass transition temperature (T_g) at 106 °C and its presence is unnoticeable as it merges with the melting temperature of blends. Melting point of C-M is lower than the P-M due to the rigid structure in crosslinked state. The formation of three dimensional structures may hinder the crystallization [6]. The crosslinked structure may restrain the growth of spherulites for the uniform arrangement of the crystalline content. Imperfect crystal formation could also contribute in the slight decrement of the melt temperature [32–35]. Fig. 4b shows the effect of MA concentration on the extent of crosslinking and melting temperature. The crosslink density, as measured from dissolution studies, increases with the concentration of MA in the blends and the maximum crosslinking is achieved 45% using 5 wt% of MA whereas the melting behaviour follow a decreasing trend.

The TGA thermograms of samples are shown in Fig. 4c. The degradation temperature (T_d) is taken as the temperature at which 5% weight loss occurs. Pure PE shows the T_d at 428 °C and ABS degrades at 301 °C. The degradation temperature of P-M and C-M are found to be 398° and 380 °C, respectively, considerably higher than pure ABS. The P-M has

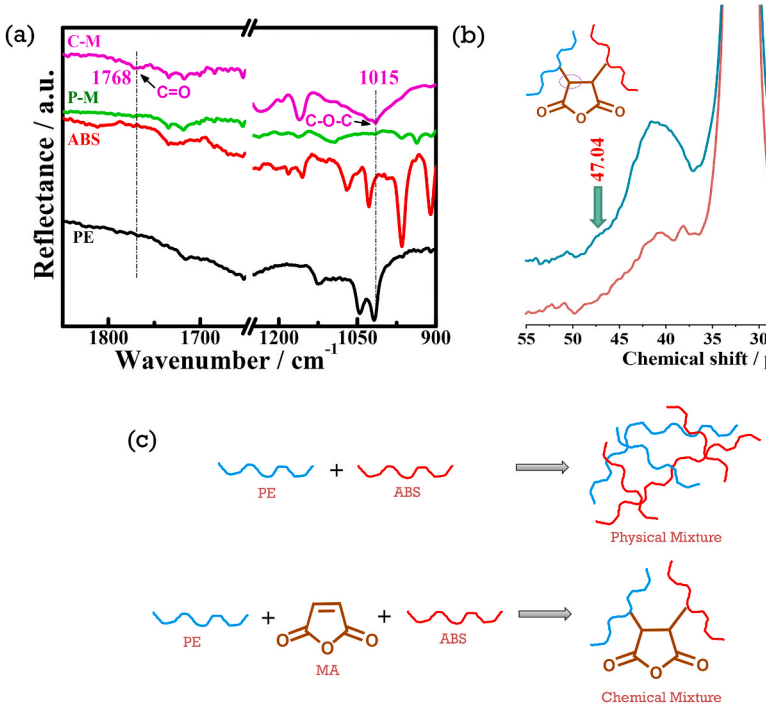

Fig. 3. Chemical bond formation due to reactive extrusion as determined through spectroscopic techniques, **(a)** FTIR spectra of indicated samples, vertical lines show the bands corresponding to chemical crosslinks; **(b)** solid state ^{13}C NMR; downward vertical line indicate the position of new peak and corresponding carbon site of crosslinking is presented on top left, inset figure on right shows the deconvolution of the peak showing prominent peak at 47.04 ppm, (for FTIR and NMR of C-M, solvent extracted parts of C-M were used); and **(c)** reaction scheme showing overlapping molecules in P-M while MA induced crosslinking is shown in C-M.

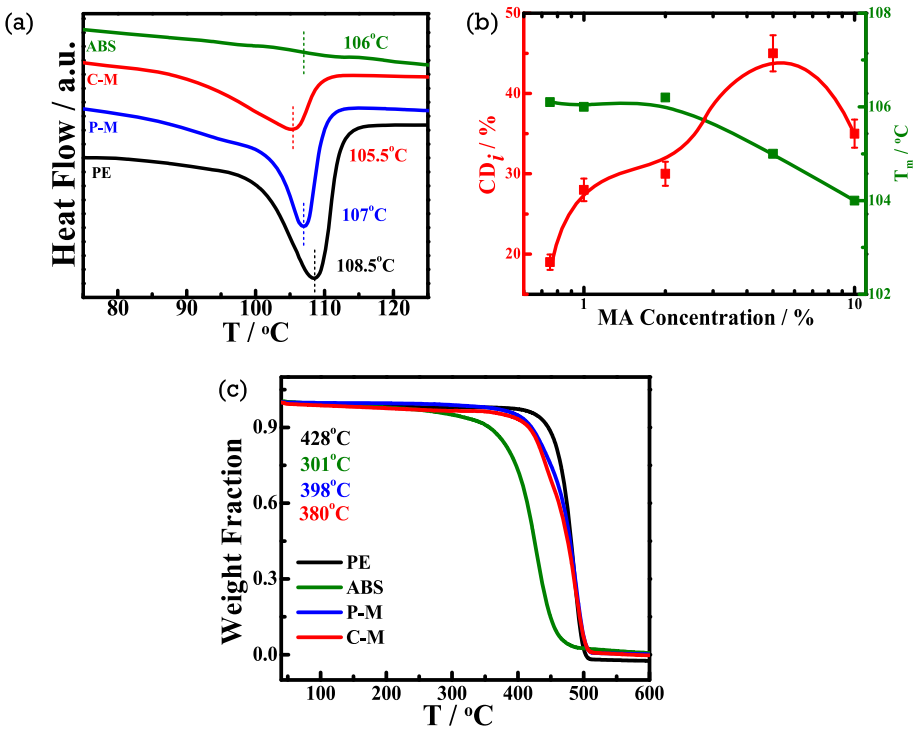

Fig. 4. **(a)** DSC thermograms of pure polymers and their indicated blends showing melting temperature; **(b)** indicative crosslink density (CD_i) and melting temperature of chemical mixture/blends as a function of MA content; and **(c)** TGA thermograms of pure polymers and their indicated blends, degradation temperatures (T_d) correspond to 5% weight loss of samples.

Table 1
Melting temperature (T_m) and degradation temperature (T_d) obtained through DSC and TGA studies.

Sample	T_m (°C)	T_d (°C) (at 5% weight loss)	T_d (°C) (at 50% weight loss)
PE	108.5	428	478
ABS	–	301	422
P-M	107.0	398	476
C-M	105.5	380	473

25 wt% ABS contributing in the decrement of the thermal property of the physical mixture. The chemical mixture shows further decrement in degradation temperature. This degradation is unlikely and may have resulted from the chain scission reactions and degradation of unreacted MAH in the C-M. At 50% weight loss, pure PE shows T_d at 478 °C whereas the P-M and C-M has T_d at 476° and 473 °C, respectively. The T_d of P-M and C-M is comparable to the pure PE, denoting that thermal stabilities of P-M and C-M are comparable with that of the PE. Presence of ABS in blends causes this slight compromise in the T_d as the ABS has T_d as low as 422 °C at 50% weight loss. The chain scission reactions taking place in C-M cause 3 °C drop in comparison to the P-M. Table 1 shows the quantitative values of melting and degradation temperature.

3.4. Mechanical properties

For the usage of blends in various applications, their mechanical performance was needed to be investigated. Fig. 5a shows the stress-strain curve of PE and its indicated blends. Young's modulus, toughness and ultimate tensile strength have been shown in Fig. 5b, c and **5d**, respectively. The quantitative values of mechanical properties have been shown in Table 2. The physical mixture shows an increment in the modulus value and considerable.

Decrease of toughness and ultimate tensile strength. On the other hand, the chemical mixture shows enhanced mechanical properties in terms of modulus and tensile strength. Toughness of C-M shows comparatively lower values as compared to PE and P-M, presumably due to lower elongation at break in crosslinked system as usual. It is noticed that modulus of P-M shows increased value of Young's modulus as compared to PE which is attributed to the inclusion of the ABS in the PE. ABS has high modulus and low toughness. The elongation at break of ABS used is as low as ~2%. The ABS particles are dispersed in PE matrix which influence the modulus of the physical mixture as the modulus of ABS is comparatively higher than PE. The embedded ABS particles strengthen the P-M until the debonding between the two phases takes place. Although, the elongation at break of P-M decreases from 104.5% to 32.6% and toughness decreases to 18.6 from 86.3 kJm^{-3} of PE. The reason for the decrement of the elongation at break of P-M is the non-uniform distribution of ABS particles in the PE matrix. Uniform dispersion and size of the dispersed phase are critical criterion for the plastic deformation in the rubber toughened polymer blends [36]. The inclusion of non-homogeneous and critically large particles results in brittle failure at the interface of the two polymers in the polymer blend. The size of the particles of the dispersed phase should not be more than a critical limit. In SEM images of fractured surface of P-M (cf. Fig. 1b), it can be seen that the ABS phase was non-homogeneously dispersed in the PE matrix. The size distribution of ABS particles was very uneven. These two factors contributed in the low values of strain at fracture. Gupta et al. [27] also related the critical domain size of the dispersed phase to the toughening of the polymer blend and reported the decrease in the elongation at break of blend at the increasing content of ABS in PP/ABS blend. Bonda et al. [17] also observed the decrease in elongation at break due to the critical parameters of the dispersed phase. The morphology of fractured surface also revealed that the ABS particles were pulled out from the PE matrix at the interface. This debonding occurred as a result of the poor interfacial adhesion. The ABS particles were pulled out from the PE matrix mostly without being broken or fractured. They left the PE polymer interface leaving a clear indent, indicating the smooth debonding. It suggests that as the P-M started to stretch, both PE and dispersed ABS. But ABS has much less toughness as

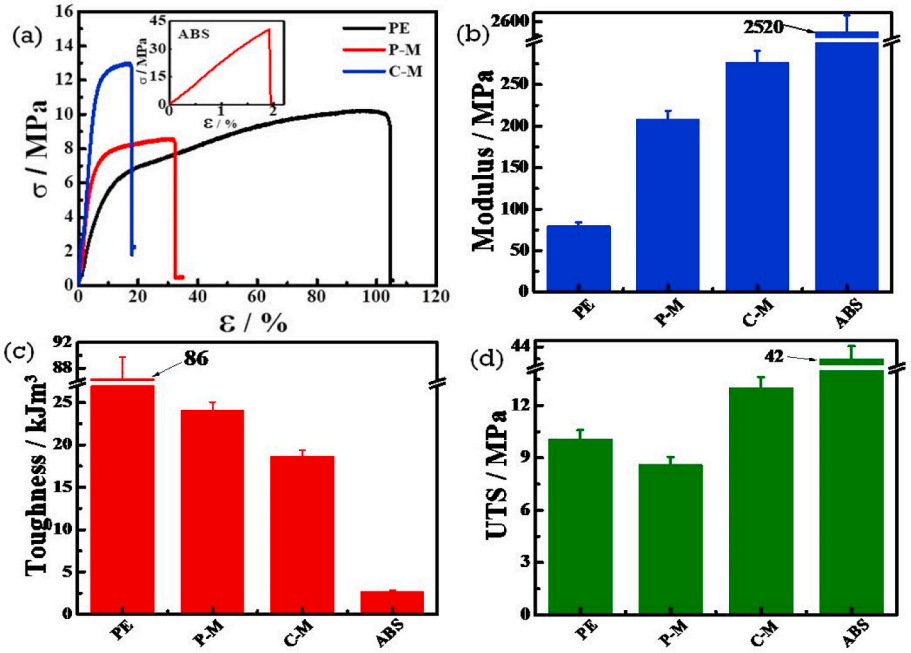

Fig. 5. Mechanical properties of pure polymers and their blends, **(a)** stress strain curves of PE, P-M and C-M, inset figure shows the stress-strain curve of E-waste ABS; **(b)** modulus; **(c)** toughness; and **(d)** ultimate tensile strength (UTS) of indicated specimens.

Table 2
Mechanical properties of pure polymers and their blends.

Sample	Young's Modulus (MPa)	Ultimate Tensile Strength (MPa)	Toughness (kJm^{-3})	Elongation at break (%)
PE	80.1 ± 4.0	10.1 ± 0.5	86.3 ± 4.3	104.5 ± 5.2
ABS	2.50×10^3 ± 126.1	42.4 ± 2.1	2.7 ± 0.1	2.1 ± 0.1
P-M	208.1 ± 9.8	8.6 ± 0.4	24.1 ± 1.2	32.6 ± 1.6
C-M	276.8 ± 10.4	13.0 ± 0.6	18.6 ± 0.9	17.7 ± 0.8

compared to PE. This difference results in the uneven stretching which created void between the two phases. The void formation led to the debonding of PE from the ABS particles' surfaces. As voids grew in size with increasing strain, the cracks developed and travelled through the blend. These cracks culminated the ultimate failure of the physical mixture. The earlier crack generation compromised the tensile strength of the physical mixture which dropped to 8.6 MPa as compared to 10.1 MPa in PE.

The chemical mixture shows the further increment in the modulus which is 246% higher than PE and 33% higher than P-M. The ultimate tensile strength of the C-M also increases to 13 MPa from 10.1 MPa of PE. The higher modulus attributes to the improved and homogeneous morphology of the C-M due to reactive blending. The ABS phase does not have the separate particles like morphology in C-M as it has in P-M. The SEM micrographs of C-M (Fig. 1b) showed a uniform miscible structure which did not have two separate phase morphology. The interaction and miscibility between two phases increase significantly in the presence of MA. The reactive extrusion of C-M cause partial crosslinking in the blend which results in the stiffened network structure in a portion of C-M. This network structure contributes in the higher modulus values in C-M. The tensile strength also increases slightly in C-M unlike physical mixture where early debonding of ABS particle and PE causes decrement in tensile strength. The elongation at break, however, decreases more than the physical mixture which is primarily due to crosslinking [4,17,37]. The reason behind this behaviour may also lie on the chain scission reactions taken place in the crosslinked blend [38].

Due to the chain scission and stiffened structure because of crosslinking, the network structure shows decreased strain at fracture and toughness. Fig. 6 depicts the three point bending test results of PE and its blends. The flexural stress-strain curve, flexural stress and flexural modulus values have been presented in Fig. 6a, b, c respectively. The bending properties of the blends are found to be improved significantly. The flexural stress increases slightly in P-M while significant improvement is noticed in P-M. The quantitative value of flexural stress of pure PE is 7.0 MPa which has increased to 8.5 MPa (21%) in P-M. On the other hand, C-M shows an increment of 83% of flexural stress value (12.9 MPa). The flexural modulus also shows the similar behaviour. The P-M exhibits an increment of 53% in the flexural modulus whereas addition of MA results in 160% improvement of flexural modulus in C-M. The developed chemical blend shows superior bending properties upon the addition of MA in minute quantity. The enhancement in bending properties is attributed to the crosslinking achieved through reactive extrusion in presence of MA. The crosslinked structure provides stiffness in C-M which results in the excellent flexural properties. P-M shows very little increment because of the poor interfacial properties between PE and ABS phase as observed in morphological studies. Therefore, it is corroborated that C-M has excellent mechanical performance to be used for various practical applications.

Dynamic Mechanical Analysis (DMA): The Mechanical properties under dynamic condition as measured through DMA provide storage modulus, loss modulus and loss tangent as a function of temperature (Fig. 7a,b,c). The storage modulus is indicative of the elastic modulus whereas the loss modulus illustrates the energy lost. The damping factor (tan δ) is calculated through the ratio of loss modulus to the storage modulus. The storage modulus variation with temperature has been shown in Fig. 7a. The G′of C-M shows increased values as compared to PE and P-M. The P-M shows decrement in storage modulus at low temperatures presumably due to immiscible interphase structure while miscible structure in C-M helps improving the stress transfer to occur smoothly. The curve of ABS shows that the storage modulus of ABS is the highest because of its high stiffness. The storage modulus results are in support of the elastic modulus data. The loss modulus variation with temperature has been presented in Fig. 7b. The two peaks represent α and β phases of LDPE. The peak at higher temperature (55 °C) represents the α phase which is indicative of motion of chains in the crystalline

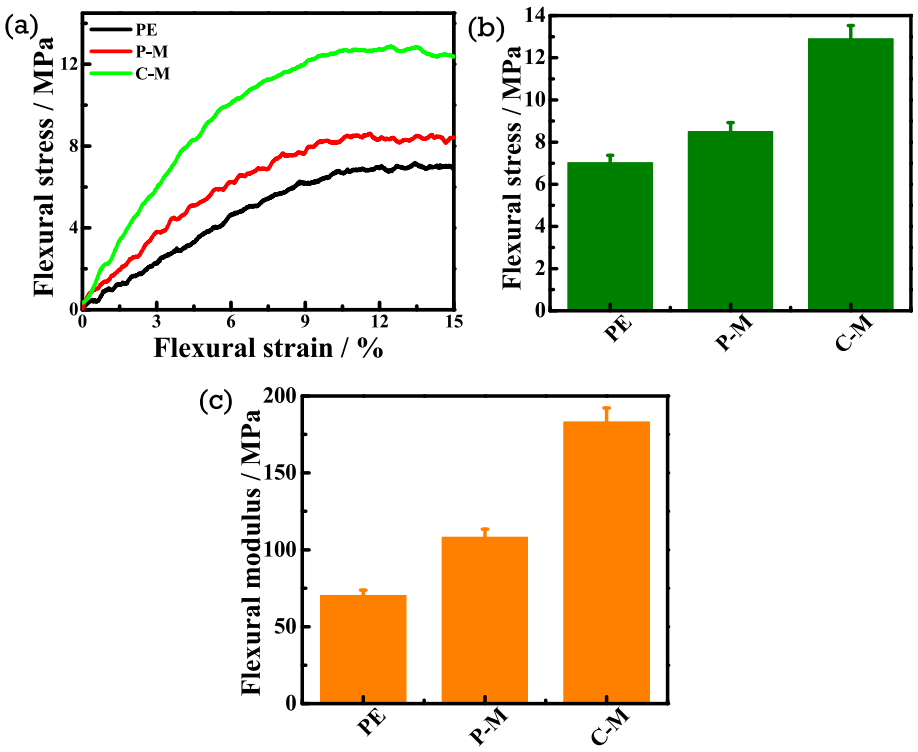

Fig. 6. Three point bending test results of PE, P-M and C-M **(a)** flexural stress-strain curves; **(b)** comparative flexural stress; and **(c)** flexural modulus showing relative increment in physical and chemical blending.

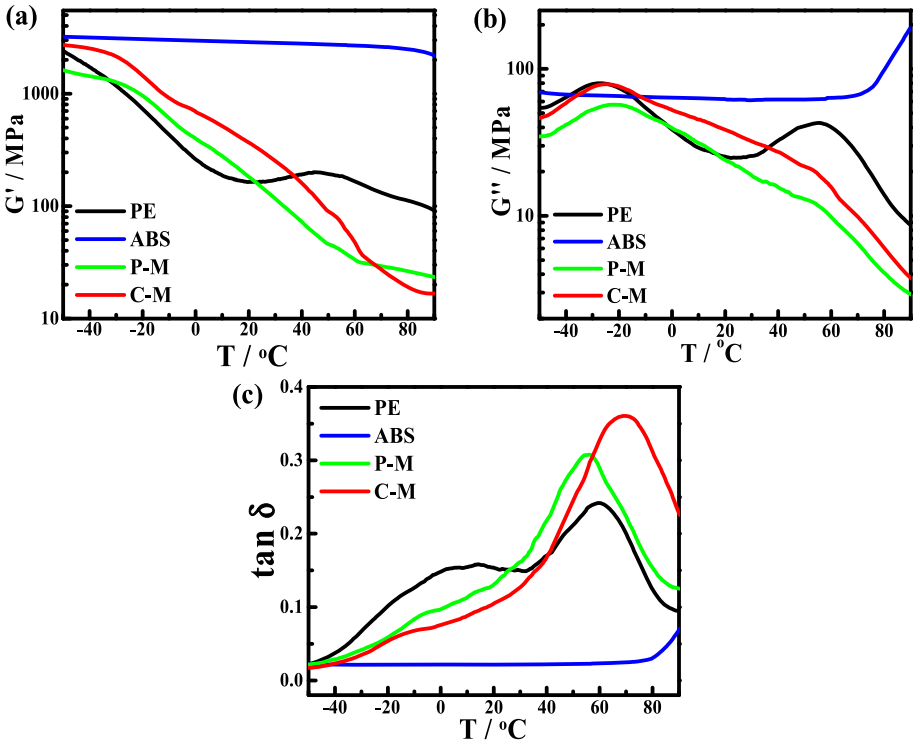

Fig. 7. Dynamic mechanical analysis of PE, its indicated blends and ABS; variation of **(a)** storage modulus; **(b)** loss modulus; and **(c)**tan δ of indicated specimens as function of temperature.

region. The peak at lower temperature (−27 °C) represents the β phase, which is associated with the molecular motion of chains in amorphous region [39]. The temperature of peak of β phase is considered as glass transition temperature [40]. Pure ABS, however, does not have these transitions with temperature variation and has a constant value curve of loss modulus till 70 °C. Due to presence of ABS phase in both the blends, amorphous part increases because of which the peak of β phase persist in P-M as well as in C-M. The crystalline content decreases considerably,

hence, the peak of α phase gets suppressed in P-M and C-M. The tan δ (loss tangent) being the ratio of loss and storage modulus, represents the contribution of both viscous and elastic parts of the material. The α peak appears in PE at 60 °C which shifts to higher temperatures in C-M. In P-M the peak temperature decreases to 55 °C but the intensity of peak increases. In C-M the peak temperature increases to 70 °C and the intensity of peak also increases. The intensity increment results due to the restriction in the movement of the polymer chains. In P-M, this restriction is posed by the embedded ABS particles. The peak intensity increases further in C-M due to the enhanced rigidity caused by greater restrictions in the polymer chains due to crosslink network present in the chemical blend which hinders the free movement considerably [39–41].

3.5. Heat distortion temperature (HDT)

The HDT is the ability to resist the significant physical deformation against temperature under load. It is a crucial parameter for the product designing as dimensional stability during the practical applications and can be affected by the thermal conditions. Hence, the polymer blends are tested at elevated temperature to determine the maximum temperature at which the blends are dimensionally stable. Fig. 8 shows the results of the heat distortion temperature. Pure PE shows a HDT of 51 °C and ABS polymer showed HDT of 78 °C. The P-M is almost as stable as PE having HDT at 53 °C. However, the HDT of C-M is found to be well above PE and P-M at 65 °C. Therefore, it is deduced that under thermal effect, the C-M shows better dimensional stability and is the most suitable for practical applications.

Chemical blend in presence of maleic anhydride (C-M) exhibits significant mechanical properties as compared to physical mixture primarily due to the crosslinking of the constituent polymer molecules and thereby forming a homogeneous structure.

4. Conclusion

The chemical mixture of LDPE and ABS have been prepared via one step reactive extrusion in a twin screw extruder in presence of 5 wt% maleic anhydride. C-M has shown enhanced properties due to the formation of crosslinked structure. SEM, POM have been used to examine the phase structural changes in crosslinked C-M. A single-phase morphology has been observed in chemical blend as comparison to two phase morphology in physical mixture prepared in absence of MA. AFM has also confirmed the change from two phase morphological structure to single phase morphology in chemical mixture. The surface roughness has been found to be decreased, indicating formation of smoother surface. Gel content has been determined via solvent extraction to observe the indicative crosslinking density. Inclusion of 5% MA found to impart the maximum crosslinking in the C-M. The structure of C-M has been examined using FTIR and solid state NMR. There are changes and shifting in the peaks of FTIR and NMR spectra which corroborates the strong chemical interactions in the chemical mixture. The chemical mixture has been found to be thermally stable although it has showed a lower degradation temperature. The Young's modulus increases up to 246% in C-M as comparison to pure PE and 33% in physical mixture. Tensile strength shows an increment of 29% in P-M as compared to pure PE. Flexural properties have also been improved and an increment of 160% has been found in flexural modulus and 83% in flexural stress. The C-M has showed 27% increment in heat distortion temperature which can be a crucial parameter in practical application where exposure of heat is prerequisite. This work has demonstrated a one-step reactive extrusion process to enhance the properties of widely used e-waste (ABS) and LDPE. Therefore, the prepared C-M has shown a way to utilize the discarded plastic by circulating it again in a useful and superior manner.

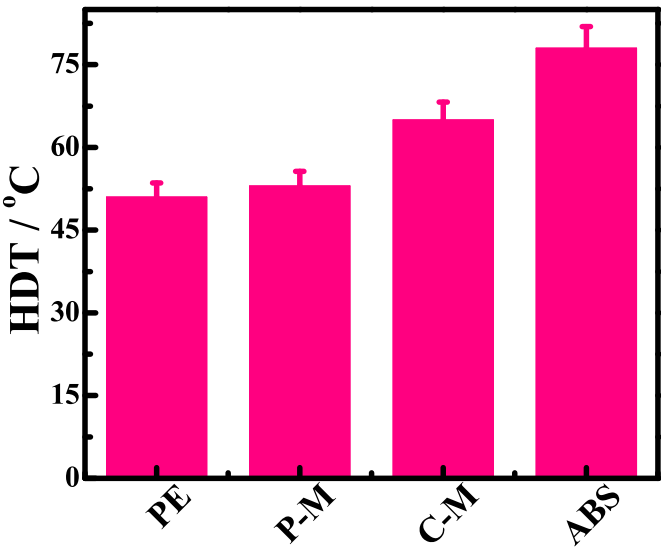

Fig. 8. Heat distortion temperature of PE, its indicated blends and ABS.

Declaration of competing interest

This is to mention that there is no conflict of interest for the manuscript entitled "Utilization of ABS from plastic waste through single-step reactive extrusion of LDPE/ABS blends of improved properties". This manuscript is solely prepared for this journal and is not being considered anywhere else for its consideration.

Acknowledgement

DS acknowledges *Indian Institute of Science, Banglore, India* for the measurements of solid state ^{13}C NMR. DS acknowledges the institute for her teaching assistantship.

Appendix A. Supplementary data

Supplementary data to this article can be found online at https://doi.org/10.1016/j.polymer.2021.123626.

References

[1] J. Bayer, L.A. Granda, J.A. Méndez, M.A. Pèlach, F. Vilaseca, P. Mutjé, Cellulose polymer composites (WPC), in: Advanced High Strength Natural Fibre Composites in Construction, Woodhead Publishing, 2017, pp. 115–139.
[2] A.A. Basfar, Z.I. Ali, Physico-chemical properties of low density polyethylene and ethylene vinyl acetate composites cross-linked by ionizing radiation, Radiat. Phys. Chem. 80 (2) (2011) 257–263.
[3] A.G. Supri, H. Ismail, The effect of isophoronediisocyanate-polyhydroxyl groups modified water hyacinth fibers (Eichhorniacrassiper) on properties of low density polyethylene/acrylonitrile butadiene styrene (LDPE/ABS) composites, Polym. Plast. Technol. Eng. 50 (2) (2011) 113–120.
[4] Q.Q. Ke, X.Y. Huang, P. Wei, G.L. Wang, P.K. Jiang, Thermal, mechanical, and dielectric behaviors of crosslinked linear low density polyethylene/polyolefin elastomers blends, J. Appl. Polym. Sci. 104 (3) (2007) 1920–1927.
[5] E.S.A. Hegazy, A.M.A. Ghaffar, H.E. Ali, Characterization and radiation modification of low density polyethylene/polystyrene/maleic anhydride/magnesium hydroxide blend nanocomposite, Mater. Chem. Phys. (2020) 123204.
[6] Z. Wang, C.M. Chan, S.H. Zhu, J. Shen, Compatibilization of polystyrene and low density polyethylene blends by a two-step crosslinking process, Polymer 39 (26) (1998) 6801–6806.
[7] T. Bremner, A. Rudin, Peroxide modification of linear low-density polyethylene: a comparison of dialkyl peroxides, J. Appl. Polym. Sci. 49 (5) (1993) 785–798.
[8] C. Xu, Z. Fang, J. Zhong, Study on phase dispersion-crosslinking synergism in binary blends of poly (vinyl chloride) with low density polyethylene, Polymer 38 (1) (1997) 155–158.
[9] M. Iqbal, C. Chuai, Y. Huang, C. Che, Modification of low-density polyethylene by graft copolymerization with maleic anhydride and blends with polyamide 6, J. Appl. Polym. Sci. 116 (3) (2010) 1558–1565.

[10] D. Saxena, N. Soundararajan, V. Katiyar, D. Rana, P. Maiti, Structural, mechanical, and gas barrier properties of poly (ethylene terephthalate) nanohybrid using nanotalc, J. Appl. Polym. Sci. 137 (27) (2020) 48607.
[11] D. Saxena, K.K. Jana, N. Soundararajan, V. Katiyar, D. Rana, P. Maiti, Potency of nanolay on structural, mechanical and gas barrier properties of poly (ethylene terephthalate) Nanohybrid, J. Polym. Res. 27 (2) (2020) 1–9.
[12] D. Saxena, D. Rana, E.B. Gowd, P. Maiti, Improvement in mechanical and structural properties of poly (ethylene terephthalate) nanohybrid, SN Applied Sciences 1 (11) (2019) 1363.
[13] A. Gaur, A. Shukla, D. Saxena, P. Maiti, Polymer composites for structural, device, and biomedical applications, Mater. Sci. Technol. (2006) 1–34.
[14] A. Shukla, P. Maiti, Biodegradable polymer-based nanohybrids for controlled drug delivery and implant applications, in: Advances in Sustainable Polymers, Springer, Singapore, 2019, pp. 3–19.
[15] K.K. Jana, C. Charan, V.K. Shahi, K. Mitra, B. Ray, D. Rana, P. Maiti, Functionalized poly (vinylidene fluoride) nanohybrid for superior fuel cell membrane, J. Membr. Sci. 481 (2015) 124–136.
[16] P. Maiti, M. Okamoto, T. Kotaka, Elongational flow birefringence of ethylene–tetracyclododecene copolymer, Polymer 42 (8) (2001) 3939–3942.
[17] S. Bonda, S. Mohanty, S.K. Nayak, Influence of compatibilizer on mechanical, morphological and rheological properties of PP/ABS blends, Iran. Polym. J. (Engl. Ed.) 23 (6) (2014) 415–425.
[18] Y.K. Lee, J.B. Lee, D.H. Park, W.N. Kim, Effects of accelerated aging and compatibilizers on the mechanical and morphological properties of polypropylene and poly (acrylonitrile-butadiene-styrene) blends, J. Appl. Polym. Sci. 127 (2) (2013) 1032–1037.
[19] P. Maiti, A.K. Nandi, Morphology of poly (vinylidene fluoride)/poly (methyl acrylate) blends: influence of chain structure, Macromol. Chem. Phys. 199 (8) (1998) 1479–1484.
[20] P. Maiti, A.K. Nandi, Influence of chain structure on the crystallization mechanism of poly (vinylidene fluoride)/poly (methyl acrylate) blends: evidence of chain extension due to blending, Polymer 39 (2) (1998) 413–421.
[21] H.G. Lee, Y.T. Sung, Y.K. Lee, W.N. Kim, H.G. Yoon, H.S. Lee, Effects of PP-g-MAH on the mechanical, morphological and rheological properties of polypropylene and poly (acrylonitrile-butadiene-styrene) blends, Macromol. Res. 17 (6) (2009) 417–423.
[22] M.A. Peydro, F. Parres, R. Navarro, S. Sanchez-Caballero, Study of the influence of adding styrene–ethylene/butadiene–styrene in acrylonitrile–butadiene–styrene and polyethylene blends, Polym. Eng. Sci. 54 (6) (2014) 1313–1324.
[23] C.K. Kum, Y.T. Sung, Y.S. Kim, H.G. Lee, W.N. Kim, H.S. Lee, H.G. Yoon, Effects of compatibilizer on mechanical, morphological, and rheological properties of polypropylene/poly(acrylonitrile-butadiene-styrene)blends, Macromol. Res. 15 (4) (2007) 308–314.
[24] R. Vadori, M. Misra, A.K. Mohanty, Sustainable biobased blends from the reactive extrusion of polylactide and acrylonitrile butadiene styrene, J. Appl. Polym. Sci. 133 (45) (2016).
[25] D. Zhao, D. Yan, N. Zhang, G. Yang, Preparation of super-toughened PA6 with submicron-sized ABS by in situ reactive extrusion method, Mater. Lett. 251 (2019) 18–22.
[26] D. Zhao, D. Yan, X. Fu, N. Zhang, G. Yang, Rheological and crystallization properties of ABS/PA6-Compatibilized blends via in situ reactive extrusion, ACS Omega 5 (25) (2020) 15257–15267.
[27] A.K. Gupta, A.K. Jain, B.K. Ratnam, S.N. Maiti, Studies on binary and ternary blends of polypropylene with ABS and LDPE. II. Impact and tensile properties, J. Appl. Polym. Sci. 39 (3) (1990) 515–530.
[28] J.G. Bokria, S. Schlick, Spatial effects in the photodegradation of poly (acrylonitrile–butadiene–styrene): a study by ATR-FTIR, Polymer 43 (11) (2002) 3239–3246.
[29] D. Lin-Vien, N.B. Colthup, W.G. Fateley, J.G. Grasselli, The Handbook of Infrared and Raman Characteristic Frequencies of Organic Molecules, Elsevier, 1991.
[30] W. Heinen, S.W. Erkens, M. Van Duin, J. Lugtenburg, Model compounds and 13C NMR increments for the characterization of maleic anhydride-grafted polyolefins, J. Polym. Sci. Polym. Chem. 37 (23) (1999) 4368–4385.
[31] R.S. Macomber, A Complete Introduction to Modern NMR Spectroscopy, Wiley, New York, 1998, pp. 97–98.
[32] Q. He, T. Yuan, X. Zhang, Z. Luo, N. Haldolaarachchige, L. Sun, D.P. Young, S. Wei, Z. Guo, Magnetically soft and hard polypropylene/cobalt nanocomposites: role of maleic anhydride grafted polypropylene, Macromolecules 46 (6) (2013) 2357–2368.
[33] V. Ojijo, S. Sinha Ray, R. Sadiku, Toughening of biodegradable polylactide/poly (butylene succinate-co-adipate) blends via in situ reactive compatibilization, ACS Appl. Mater. Interfaces 5 (10) (2013) 4266–4276.
[34] Q. Wang, H. Chen, Y. Liu, LDPE-g-MAH prepared through solid-phase mechanochemistry and its compatibilizing effects on HDPE/CaCO3, Polym. Plast. Technol. Eng. 41 (2) (2002) 215–228.
[35] M. Saroop, G.N. Mathur, Studies on dynamically vulcanized polypropylene (PP)/ butadiene styrene block copolymer (SBS) blends: crystallization and thermal behavior, J. Appl. Polym. Sci. 71 (1) (1999) 151–161.
[36] S.C. Wong, Y.W. Mai, Effect of rubber functionality on microstructures and fracture toughness of impact-modified nylon 6, 6/polypropylene blends: 1. Structure–property relationships, Polymer 40 (6) (1999) 1553–1566.
[37] J. Morshedian, H.A. Khonakdar, M. Mehrabzadeh, H. Eslami, Preparation and properties of heat shrinkable crosslinked lowdensity polyethylene, Adv. Polym. Technol.: Journal of the Polymer Processing Institute 22 (2) (2003) 112–119.
[38] G. Moad, The synthesis of polyolefin graft copolymers by reactive extrusion, Prog. Polym. Sci. 24 (1) (1999) 81–142.
[39] D.E. Kline, J.A. Sauer, A.E. Woodward, Effect of branching on dynamic mechanical properties of polyethylene, J. Polym. Sci. 22 (102) (1956) 455–462.
[40] J.A. Molefi, A.S. Luyt, I. Krupa, Comparison of the influence of copper micro-and nano-particles on the mechanical properties of polyethylene/copper composites, J. Mater. Sci. 45 (1) (2010) 82–88.
[41] J. Jyoti, B.P. Singh, A.K. Arya, S.R. Dhakate, Dynamic mechanical properties of multiwall carbon nanotube reinforced ABS composites and their correlation with entanglement density, adhesion, reinforcement and C factor, RSC Adv. 6 (5) (2016) 3997–4006.